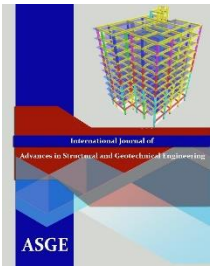

International Journal of Advances in Structural and Geotechnical Engineering

https://asge.journals.ekb.eg/

Print ISSN 2785-9509 *Online ISSN 2812-5142*

Special Issue for ICASGE'19

FLEXURAL BEHAVIOUR OF COMPOSITE REINFORCED NSC/SHCC DECK SLABS

Mohamed A. Kassem, Tarek F. El-Shafiey, Mohamed H. Mahmoud, Hamdy M. Afefy and Ali Hassan2

ASGE Vol. 04 (04), pp. 40-58, 2020

International Conference on Advances in Structural and Geotechnical Engineering

ICASGE'19

25-28March 2019, Hurghada, Egypt

Flexural behaviour of composite reinforced NSC/SHCC deck slabs

Mohamed A. Kassem[1], Tarek F. El-Shafiey[1], Mohamed H. Mahmoud[1], Hamdy M. Afefy[1*] and Ali Hassan[2]

ABSTRACT

In order to expand the life-time as well as to eliminate some drawbacks associated with the use of traditional normal strength concrete in bridge construction, a new composite NSC/ SHCC deck slab is proposed and investigated. The superior tensile characteristics of the Strain Hardening Cementitious Composites (SHCC) could be engineered when a thin layer of such material is used in the tension side of the deck slab. The effects of reinforcement ratio of the main steel as well as the thickness of the substrate SHCC layer have been studied. Five composite NSC/SHCC slab specimens along with two control specimens made of normal strength and high-performance concrete were prepared and tested. The responses of all specimens have been compared from the viewpoint of ultimate capacity, developed ductility and cracking characteristics. The experimental results showed that the proposed NSC-SHCC deck system was found to have enhanced performance with regard to flexural capacity and serviceability, compared to the conventional reinforced concrete deck. The increase of the SHCC thickness had little effect on the cracking, yielding, and ultimate loads, while a considerable enhancement in the post-cracking behaviour was obtained with the increase of reinforcement ratio.

Keywords: Bridges; crack width and spacing; composite deck slab; failure; Strain Hardening Cementitious Composites (SHCC).

INTRODUCTION

Cracking in reinforced concrete (RC) members is one of the most important factors that affect the durability of such members [1]. Wider cracks can permit the chemical reaction to activate the oxidation of the surface of the steel reinforcing bars. Consequently, controlling the developed crack width is essential to prevent reinforcement corrosion [2]. Furthermore, visible and wide cracks affect the aesthetics appearance of the RC structure which provokes negative criticism.

In order to eliminate the drawback of the developed cracks on the tension side of the conventional concrete bridge decks, the design of reinforced concrete sections must assure that the maximum crack width under service load conditions is under the permissible limits. Most of design codes recommend the allowable crack width under service to be in the range of 0.2-0.3 mm [3 - 6], for structures exposed to high humidity and moisture conditions such as RC bridges. Moreover, the crack width should not be more than 0.2 mm for exposed to deicing chemicals. Limiting the crack width under definite range can effectively reduce the durability problem; nonetheless this comes at the expense of the maximum allowed service loads [7].

Fiber Reinforced Polymer (FRP) with concrete topping hybrid decks been adopted as a promising solution to enhance durability and increase load-carrying capacities of bridge decks. That is because the enhanced characteristics of the FRP materials such as high tensile strength, ease of installation, lightness, good electromagnetic insulation properties, and almost no need to maintenance requirements [8, 9]. However, the main problems of the FRP-concrete composite decks are the low stiffness of the FRP deck in the direction of the main girder and the FRP brittle behavior along with the insufficient interfacial shear capacity to develop the full composite action between the FRP plates and the topping concrete [10]. Accordingly, the use of FRP-concrete hybrid deck was hindered.

Strain Hardening Cementitious Composite (SHCC) is a new generation of fiber-reinforced cementitious composites that consists of sand, cement, fly ash, silica fume, and short fibers [11-16].The SHCC material exhibits a pseudo strain hardening behavior characterized by the formation of multiple fine cracks under tensile loading. Characteristics of multiple cracking of the SHCC could enhance both the durability and impermeability properties of this material [17-24]. When the SHCC material was used in repair applications, it showed a considerable high tensile strain capacity, which is a main important criterion of a durable material in order to resist premature failures [25-27].

In the current study, a new generation of composite bridge deck system is proposed that is expected to overcome many problems associated with the use of conventional concrete in bridge decks. Utilizing a thin pre-cast layer of SHCC as a permanent shuttering in partial-depth pre-cast concrete deck is expected to be an effective and promising construction technique. This is because the use of partial depth pre-cast bridge deck could safe construction cost. Furthermore, the superior tensile characteristics of the SHCC could enable the composite deck slab to improve its overall structural performance in terms of flexural capacity, serviceability, durability, corrosion resistance and permeability.

This study proposes and verifies the applicability of a new composite deck slab in the bridge construction in order to improve the overall structural performance as well as to eliminate some drawbacks associated with the use of conversional concrete. Seven simply supported composite bridge decks are configured and casted in order to investigate the effect of reinforcement ratio of the main tensile steel and the thickness of the SHCC layer on the failure load, cracking load, the load-deflection response, cracks spacing and major crack width of on their overall structural performance. And then compare such performance with that of traditional normal strength concrete deck slabs.

EXPERIMENTAL WORK PROGRAM

Test specimens

The experimental work program consisted of seven typical bridge deck slabs divided into three groups. All slab specimens had the same concrete dimensions of 800 mm width, 220 mm thickness and a total length of 2400 mm, while the center-to-center span was 2000 mm.

Group (I) contained three specimens; the first one was made of normal strength concrete (NSC), the second one was made of high performance concrete, and the last had a composite NSC/SHCC section that was combining normal strength concrete toping and pre-cast strain hardening cementitious composites layer of 50 mm thickness at the tension side while the reinforcement ratio of the main tensile steel was kept constant (0.68%). All specimens of group (II) had similar configuration and reinforcement of the composite section of group (I) except that the thicknesses of SHCC layer was switched to be either 70 mm or 90 mm. The specimens of group (III) had SHCC layer of 50 mm thickness while main steel reinforcement ratio was changed to have two different tensile reinforcing ratios of 0.38% and 0.86%.

It is worth mentioning that the thickness of SHCC layer of all specimens was selected to satisfy the concrete cover requirements for exposed reinforced concrete structures. In addition, the used flexural reinforcement ratios (0.38%, 0.68% and 0.86%) were selected to guarantee the tension-controlled failure according to the current ECP 203-2017[5] and ACI 318-14[6] codes.

Table 1 summarizes the characteristics of all specimens along with the objectives of each test group, while the concrete dimensions and the reinforcement detailing of the control normal strength concrete specimen and the typical NSC/SHCC specimens are depicted in Figs. 1 and 2, respectively.

2.2 Manufacturing of composite NSC/SHCC specimens

All composite NSC/SHCC specimens were cast using the same SHCC mix and followed the same casting procedure. The specimens were cast in two stages. In the first stage, the SHCC layer was cast in to wooden molds after positioning of longitudinal and transverse bottom reinforcing bars (Fig. 3(a)). The reinforcing seats were placed prior to casting of SHCC layer not only to support the upper reinforcing mesh but also to resist the developed interfacial shear stress between the SHCC layer and NSC toping (Fig. 3(b)). The SHCC material has self-consolidating characteristics; no internal or external vibrations were applied during the casting. SHCC was poured from one end of the formwork and was allowed to flow to the other end. Whenever more material was required, it was poured behind the leading edge of the flowing material. The same casting method was used for all specimens to maintain a similar fiber distribution. The pre-cast SHCC layers were de-molded after 24 hours and cured under wet conditions for two weeks (Figs. 3(c) and (d)).

After two weeks of curing for the SHCC substrate, the reinforcing bars were prepared and assembled for the second stage of casting (Fig. 3(e)).In the second stage, the NSC topping was cast and leveled to have the final NSC/SHCC composite section (Fig. 3(f)). All test specimens were cast at the same time horizontally in wooden forms using a ready-mix concrete to assure quality control during the fabrication of the test specimens. The upper surface of all specimens were cured by wet sackcloth for two weeks, and then allowed air-drying until the testing day.

Material Properties

The used NSC patch was a ready mix concrete of 28-day cube compressive strength of 30 MPa. For the SHCC material, the water-to-binder ratio (W/B) was kept 0.20. Ordinary Portland cement having a density of 3.14 g/cm3 was used, and 15% of the design cement content was replaced by silica fume. Quartz sand with a diameter less than 0.5 mm was used as a fine aggregate while high strength Polypropylene (PP) fiber was chosen for the SHCC and its volumetric ratio was 2.0%. The average cylindrical compressive strength at the age of 28 days was designed to be 50 MPa, more details about the design mix and its tensile as well compressive properties can be found elsewhere[28].

Test setup and procedure

The experimental test program was performed under the testing frame of the Reinforced Concrete Laboratory of the Faculty of Engineering, Tanta University as shown in Fig. 4(a). All test specimens were loaded using three point bending scheme. The specimen ends were simply-supported over roller support at one end and hinged support at the other end. All specimens were tested under an incremental static patch load applied at the mid-span region of test specimen, simulating the AASHTO truck wheel foot print of 20 x 10 in. (508 x 254 mm) for an HS-20 truck dual-tire wheel, using a rigid steel spreader beam as depicted in Fig. 4(b). A laser level was used to ensure the coincidence of the axes of test specimen, the load cell and the loading beam before testing.
A 100 mm linear variable displacement transducer (LVDT) was used in order to measure the vertical deflection at mid-span point of the slab, while, 10 mm strain gauges were used in order to measure the developed normal strains in the internal reinforcement at the tension side. Also, a series of 100 mm gauge length Pi gauges were used to measure the developed strain on the concrete surface along the depth of the specimen at mid-span. An optical microscope of 0.01 mm accuracy was used in order to measure the major crack width. The major crack width was measured at four different stages; namely, at first cracking of concrete at tension side, corresponding to the service load level, corresponding to the yielding load of the internal reinforcement, and near failure. Moreover, the inspection of the minor invisible cracks was carried out using a magnifying glass.The acting patch load was applied at different steps at 10 kN increment in order to allow for visual inspection of the specimen and to mark the developed cracks. The acting load was measured by a load cell of 600 kN capacity. After each loading step, the vertical deflection, the developed normal strains in the longitudinal steel bars as well as on developed deformations on the concrete surface were recorded and stored by an automatic data logger unit (TDS-150).

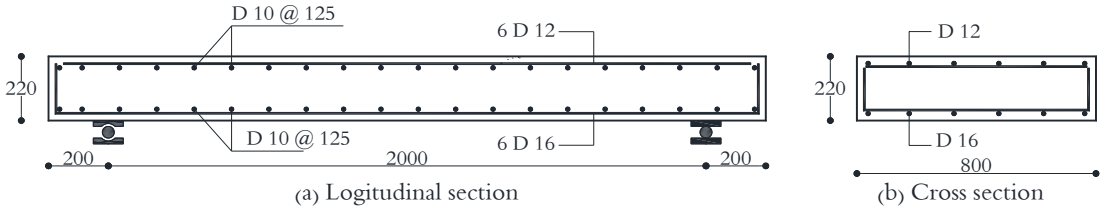

Fig. 1Concrete dimensions and reinforcement detailing of control specimens SN $_{0.68\%,0.}$

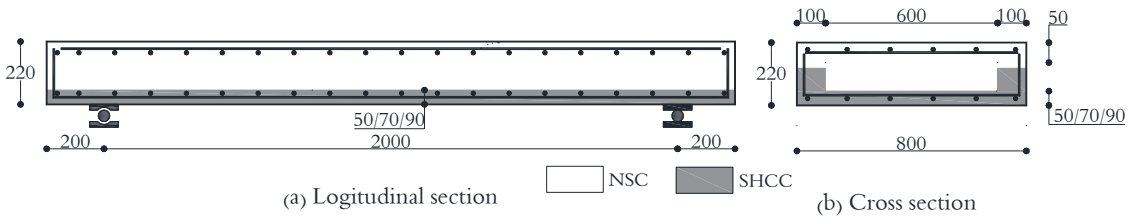

Fig. 2 Concrete dimensions and reinforcement detailing of composite NSC-SHCC specimens.

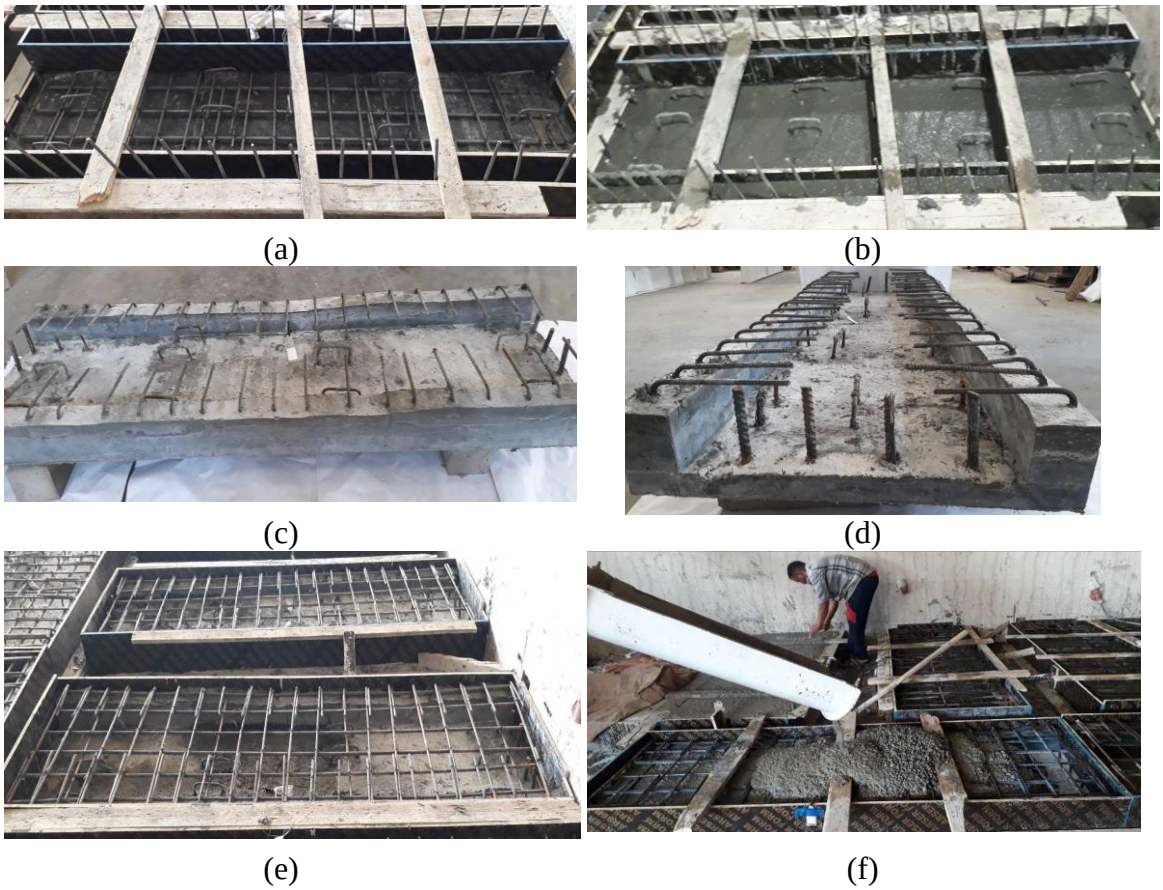

Fig. 3 Fabrication process of test specimens: (a) Placing of bottom reinforcement before casting SHCC layer; (b) Panel after casting of SHCC layer; (c) Plan view of precast SHCC panel; (d) Side view of precast SHCC panel; (e) Composite panels after placing of upper reinforcing mesh; (f) Casting of NSC topping.

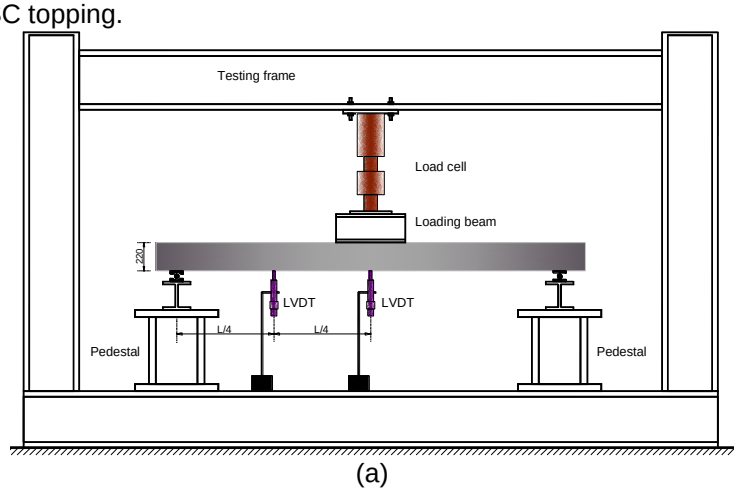

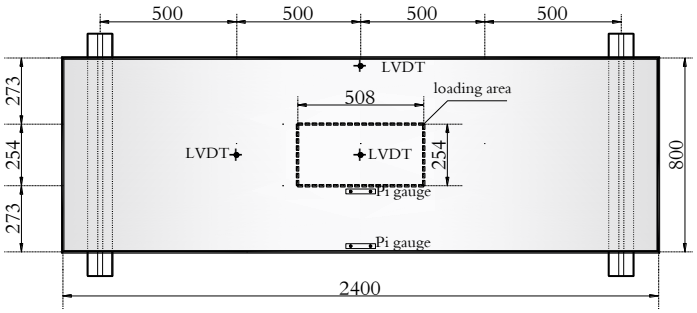

(b)

Fig. 4 Typical setup and instrumentations: (a) elevation;(b) plan

Table 1: Experimental program

Objectives	Reinforcement		Thickness (mm)		Specimen	Group No.
	Top	Bottom (μ %)	SHCC	NSC		
Study the effect of material type	6 D 12	6 D 16 (0.68%)	-	220	$SN_{0.68\%,0}$	Group (I)
	6 D 12	6 D 16 (0.68%)	-	220	$SH_{0.68\%,0}$	
	6 D 12	6 D 16 (0.68%)	50	170	$SC_{0.68\%,0}$	
Study the effect of reinforcement ratio	6 D 12	6 D 12 (0.38%)	50	170	$SC_{0.38\%,50}$	Group (II)
	6 D 12	6 D 18 (0.86%)	50	170	$SC_{0.86\%,50}$	
Study the effect of SHCC thickness	6 D 12	6 D 16 (0.68%)	70	150	$SC_{0.68\%,70}$	Group (III)
	6 D 12	6 D 16 (0.68%)	90	130	$SC_{0.68\%,90}$	

SN = normal strength concrete specimen; SH = high performance concrete specimen; SC = composite NSC/SHCC specimen; μ = reinforcement ratio = area of main steel / area of cross section.

RESULTS AND DISCUSSIONS

In order to verify the adequacy of the proposed composite NSC/SHCC section for the bridge deck slab, a detailed discussion for the behavior of all test specimens in terms of ultimate loads, failure modes, load deflection behavior, and cracking behavior is provided.

CRACKING PATTERN AND MODES OF FAILURE

During testing of specimens, the cracks were marked after each load increment. The numbers next to the cracks refer to the load (in kN units) at which the cracks were first observed. After the collapse, failure cracks were marked and the specimens were photographed. The progress of cracking provided useful information regarding the failure mechanism of the specimens.

Group (I) consists of three bridge deck specimens with constant reinforcement ratio. These specimens were tested up to the failure to evaluate the flexural performance of the proposed NSC/SHCC composite bridge deck in comparison with normal strength and high-performance bridge decks .

For specimen SN0.86%,0 that was made of normal strength concrete, the initial crack started to appear near the mid-span section of the specimen at a vertical load of about 54 kN. With further loading, the cracks spread from the mid-span section to the supporting section with crack spacing of 50–200 mm. After yielding of the main tensile steel, the crack widths greatly increased. Proceeding of loading resulted in the cracks extended upward, which indicates a large upward shift of the neutral axis after yielding of the internal steel reinforcement. Accordingly a slight increase of the carried load after yielding of internal reinforcement was recorded. Substantially high compressive stress was generated through force equilibrium.

Crushing of the concrete in a shallow layer became noticeable with increasing deformation of the specimen, without further increase of applied load. Finally, the failure of the specimen was controlled by concrete crushing at the top of the specimen, which is a typical failure pattern of under-reinforced flexural members as depicted in Fig. 5 .

For the HPC specimen, SH0.68%,0, the presence of internal fibers in concrete has greatly affected the observed cracking pattern as depicted in Fig. 6.The cracks of HPC specimen were spaced more closely in comparison with that developed in the NSC specimen. The HPC specimen SH0.68%,0 exhibited flexural cracks with short depths in comparison with those of specimen SN0.68%,0 made of normal concrete. The propagation of cracks was effectively restrained by fiber bridging at the crack surfaces. However, the HPC exhibited a continuous increase in the number of cracks approaching the peak load along with an insignificant increase in the crack widths. In addition, most of the cracks gradually propagated into the compression zone and the cracks were not visually widened. This observation indicates that the HPC is able to redistribute the tensile stresses before the fiber pullout. After the yield load, the fibers at one or two specific cracks began to pull out, and then the width of these specific cracks increased significantly compared to those of other cracks (this phenomenon is well known as crack localization). The specimen failed, as expected, in flexural mode with extensive yielding of the tension steel, followed by crushing of the concrete in the compression zone.

The failure of composite NSC/SHCC specimen SC 0.68%,50 was similar to that of specimen SH0.68%,0 made of High-performance concrete. For the composite specimen SC0.68%,50, an initial crack was observed near the mid-span section on the SHCC layer at a vertical load of about 100 kN. Approaching the yield load, the major crack width was slightly increased; nevertheless, a multiple micro-cracks were observed along the entire tensile side of the tested specimen. After yielding of the main reinforcing steel bars and before concrete crushing, the fibers began to pull out, and then the width of some specific cracks increased significantly compared to those of other cracks due to crack localization. Furthermore, the specimen gradually lost about 15% of the achieved ultimate load, which represent the contribution of SHCC material to the ultimate load. Finally, the specimen failed after crushing the concrete at the compression side, which is similar to that of specimen SH0.68%,0, but with a noticeable increase in the crushed zone as depicted in Fig. 7. The most important observation for SH0.68%,0 was that after the complete failure, no detachment between the concrete topping and the SHCC layer was noticed. A complete bond between both of them was maintained during all loading stages. Moreover, during the overall process of loading, no shear cracks were noticed.

Varying the reinforcement ratio of the main tensile steel keeping it below the maximum permissible ratio did not affect the crack distribution as well as the manifested mode of failure as exhibited by all specimens of group (II) after complete flexural failure as depicted in Fig. 8. Similarly, increasing the thickness of substrate SHCC layer as implement in all specimens of group (III) did not alter the final cracking pattern as well as the mode of failure as shown in Fig. 9 .

Table 2: Acting load, corresponding mid-span deflection for all specimens at different loading stages.

Group No.	Specimen	P_{cr} (kN)	Δ_{cr} (mm)	P_s (kN)	Δ_s (mm)	P_y (kN)	Δ_y (mm)	P_u (kN)	Δ_u (mm)
Group (I)	$SN_{0.68\%,0}$	54	1.20	200	6.65	250	7.12	291	40.10
	$SH_{0.68\%,0}$	82	1.50	216	6.15	270	8.10	324	33.20
	$SC_{0.68\%,50}$	100	1.70	240	6.05	300	7.20	364	22.10
Group (II)	$SC_{0.38\%,50}$	98	1.65	176	5.08	220	7.00	259	18.10
	$SC_{0.86\%,50}$	102	1.75	292	5.58	365	7.25	425	25.50
Group (III)	$SC_{0.68\%,70}$	102	1.68	244	5.50	305	7.15	381	21.25
	$SC_{0.68\%,90}$	105	1.65	248	5.42	310	7.10	390	22.20

P_{cr} = cracking load; Δ_{cr} = central deflection corresponding to cracking load; Ps = Service load corresponding to 0.8fy of the tension steel; Δs = central deflection corresponding to service load; P_y = yielding load when the load-deflection curve begins to deform plastically; Δ_y= central deflection corresponding to yielding load; P_u= ultimate load; Δ_u= central deflection corresponding to ultimate load

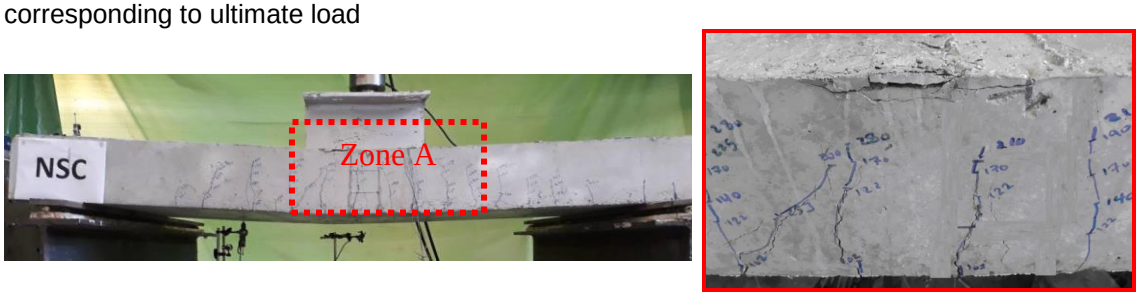

Fig. 5 Final crack pattern of specimen $SN_{0.68\%,0}$.

Fig. 6 Final crack pattern of specimen $SH_{0.68\%,0}$.

Fig. 7 Final crack pattern of specimen $SC_{0.68\%,50}$.

Fig. 8 Final crack pattern of specimens of group (II).

Fig. 9 Final crack pattern of specimens of group (III).

CRACKING AND ULTIMATE LOADS

Table 2 summarizes the acting loads along with their corresponding mid-span deflections at different stages of loading. Experimental results show that using high-performance concrete resulted in delaying the appearance of the first flexural compared to that of the normal strength concrete slab. The percentage of increase in the first cracking load is about 52% for specimen SH0.68%,0 compared to that of the specimen SN0.68%,0. In addition, using composite NSC/SHCC section enabled the deck slab to crack at higher load compared to that odf specimen SH0.68%,0 . The percentage of increase in the first cracking load is about 85% for specimen SC0.68%,0 compared to that of the specimen SN0.68%,0.It could be concluded that the pre-cast SHCC layer effectively reduced the initial crack tendency.

Based on the recorded values of the ultimate load carrying capacities for the tested specimens as listed in Table 2, it can be observed that the ultimate load capacity of the high-performance concrete specimen SH0.68%,0is higher than that of the normal strength concrete specimen SN0.68%,0 by about 11%. That could be attributed to the enhanced characteristics of HPC in tension and compression compared to those of conventional normal strength concrete. Using composite NSC/SHCC section enabled the specimen to sustain higher ultimate load compared to that of the specimen made of high-performance concrete. The specimen SC0.68%,50 showed higher ultimate capacity by about 25% and 12 % compared to that of specimens SN0.68%,0 and SH0.68%,0, respectively. That can be attributed to the contribution of the 50 mm thick SHCC pre-cast layer to tension reinforcement.

Effect of reinforcement ratio on cracking and ultimate loads

Based on the results in Table 2, it can be noticed that the cracking load was slightly increased with the increase of reinforcement ratio. The test specimens of group (II) exhibited almost the same flexural cracking loads, which are 98 kN, 100 kN, and 102 kN for specimens SC0.38%,50, SC0.68%,50, and SC0.86%,50, respectively, having reinforcement ratios of 0.38, 0.68 and 0.86%. This is confirming that the cracking load is mainly dependent on the SHCC tensile characteristics of specimens, while the internal main steel reinforcement ratio has insignificant effect. On the other hand, increasing the main steel reinforcement ratio resulted in increasing the ultimate load significantly. The percentages of increases in the ultimate capacities are 40 and 64%, respectively for specimens SC0.68%,50 , andSC0.86%,50, having reinforcement ratios of 0.68% and 0.86%, compared to that of specimen SC0.38%,50, which has reinforcement ratio of 0.38% .

Effect of the thickness of the SHCC layer on cracking and ultimate loads

Increasing the thickness of the SHCC layer of specimen SC0.68%,90 to 90 mm which is 80% higher than that provided to specimen SC0.68%,50, resulted in increase the cracking load by about 5%. The slight increase in the cracking load does not fit to the cost of increase in the SHCC layer. This result highlights that the sufficient SHCC thickness required to outperform the cracking characteristics of NSC/SHCC composite bridge decks is 50 mm for the tested specimen which is 0.25% of section depth.

Comparatively, the ultimate loads of NSC/SHCC specimens were increased by increasing the SHCC thickness. The recorded ultimate capacities were 381 kN, and 390 kN, respectively, for

specimens SC0.86%,70, and SC0.86%,90.Consequently, the percentage of increases in ultimate capacities are about 5%, and 7% compared to that of specimen SC0.68%,50. it can be noticed that the enhancement in ultimate capacity is more than the enhancement in cracking load due to increase the thickness of the SHCC layer, and this reflects the fact that the strain hardening of SHCC arises beyond crack occurrence.

LOAD-DEFLECTION BEHAVIOR

The load-deflection curve for all specimens of the group (I) is shown in Fig. 10. According to the recorded load-deflection curve of specimen SN0.68%,0 made of normal strength concrete, this relationship could be divided into four main stages as depicted in Fig.11(a).The initial stage began with the commencement of testing till the appearance of the initial crack, which was denoted as Point 1. The specimens behaved almost linearly at this stage. When the load reached about 30% of the ultimate load, the first crack was observed and the stiffness decreased obviously after cracking. The second stage began from the initial cracking to the yielding load of the main tensile steel, which was a turning point of the load-deflection curve shown as Point 2. The yield stage began from the yield load till the maximum load, which was denoted as Point 3. More cracks appeared, and the crack width increased as the load increased. The failure stage began with the maximum load and continued until the complete failure of the specimens occurred. The deflection increased as concrete crushing and load-bearing capacity decreased.

On the other hand, the NSC/SHCC specimen behaved almost at a similar trend till the cracking load. Beyond the cracking load, fibers effectively controlled the increase in crack widths, and multiple micro-cracks were formed due to the fiber bridging at crack surfaces, leading to strain-hardening response. Therefore, it can be noticed that the strain-hardening of SHCC effectively controlled the degradation of post-cracking stiffness of specimen SC0.68%,50 in comparison with specimen SN0.68%,0 that was made of normal strength concrete. Also, after the composite specimen SC0.68%,0 reached its ultimate load, the specimen was able to sustain inelastic deformation prior to collapse, without significant loss in resistance. Before concrete crushing, the curve showed a softening tail (tension softening curve), and the load drops gradually from the peak load to a load level around that developed by the normal strength concrete specimen owing to the loss of the fibers contribution (Fig.11(b).

Effect of reinforcement ratio on load-deflection response

Fig. 12 shows the load-deflection response for the test specimens of group (II) as well as the specimen SC0.68%,0 that was reinforced with 0.68% reinforcement ratio. Specimens SC0.38%,50 and SC0.86%,50, were provided with 0.38% and 0.86% reinforcement ratio, respectively. All specimens showed approximately the same response till the cracking load. After the beginning of the first flexural crack, the effect of reinforcement ratio was apparent, as with increasing reinforcement ratio the specimen was able to form less deflection at the same loading level. Furthermore, after the specimens reached their ultimate loads, all specimens were able to sustain inelastic deformation prior to the collapse, without significant loss in resistance. Also, the sustained inelastic deformation was increased by increasing reinforcement ratio. After the specimens reached their ultimate load, and prior to crushing of concrete at compression zone, the curve demonstrated a softening tail (tension softening curve), and the load drops gradually from the peak to a load level around that can be resisted by reinforcing bars .

Effect of the thickness of the SHCC layer on load-deflection response

The test results indicated that, at the first stages of loading, there was a negligible influence of increasing the thickness of the SHCC layer on the flexural performance of NSC/SHCC composite section as depicted in Fig. 13. For all specimens of group (III), the load-deflection curves could go up identical till yielding of internal reinforcement, but once yielding happened, the increase in SHCC thickness slightly affected the recorded deflection. The possible reason for this was that, increasing the SHCC thickness diminished the flexural crack propagation after yielding of internal reinforcement, thus decreased the rate of stiffness degradation which enabled the NSC/SHCC specimen to sustain higher load.

It is worth mentioning that, all specimens of group (III) showed a similar post-peak behavior, which distinguished by inelastic deformation followed by a gradual decrease of load carrying capacity to a load level around that achieved by the control normal strength concrete specimens SN0.68%,0 .

LOAD-STRAIN BEHAVIOUR

Figure 14 shows the development of the normal strain on the main tensile steel bars along the entire loading course for specimens $SN_{0.68\%,0}$, $SH_{0.68\%,0}$, and $SC_{0.68\%,0}$. In all specimens, the relationship of the load-strain could be described by a tri-linear relationship. The first part of this relationship exhibited linear behavior up to the occurrence of the first crack, beyond which a rapid change in the slope of the load–strain curve was observed. By further loading, the yielding of the internal steel reinforcement occurred and then a steady plateau in the load-strain curve was observed soon after that till the complete failure of the specimen. For all specimens, strains are almost the same at loads below cracking of the concrete. After cracking, there was significant change in the steel bar strain among all specimens. This difference may be attributed to fibers bridging mechanism that can effectively distribute the cracks, and prevent strain localization. Moreover, it was observed that $SC_{0.68\%,0\%}$ exhibited lower strainat the same load level compared with that exhibited by $SN_{0.68\%,0}$ and $SH_{0.68\%,0}$.

Regarding the yielding load, the combination of SHCC layer and steel bars in tension side increased the yielding load of specimen $SC_{0.68\%,50}$by about 20%, and 11% compared with that of specimens $SN_{0.68\%,0}$ and $SH_{0.68\%,0}$, respectively. This reflects the ability of utilization of SHCC layer in tension side to reduce the reinforcement ratio in bridge deck construction.

Effect of reinforcement ratio on load-strain behaviour

The measured normal strain on the middle reinforcing bar versus the acting load of the tested specimens of the group (II) is depicted in Fig. 15. All specimens showed a similar trend of load versus strain curves. However, increasing the reinforcement ratio of the main tension steel resulted in decrease the developed strain at the same loading level. The developed strains on the main steel exceeded its yielding strain, and the stiffness was generally stabilized at a constant rate. That happened for all specimens of group (II). Generally, the increase of reinforcement ratio significantly increased the yielding load. The yielding loads are 220 kN, 300 kN, and 365 kN for specimens $SC_{0.36\%,50}$, $SC_{0.68\%,50}$ and $SC0.86\%,50$, respectively.

Effect of the thickness of the SHCC layer on load-strain behavior

The test results indicated that there was an insignificant influence of the increase of the SHCC thickness on the flexural performance of the composite deck except the post-yielding stage of loading as depicted in Fig. 16. From the beginning of loading till the occurrence of yielding, all specimens showed approximately a similar load versus strain curves. After that the response of load-strain relationship is slightly affected by the increase of SHCC thickness. Specimen $SC_{0.68\%,50}$ which provided by 50 mm thick SHCC layer was the most affected by main steel yielding, therefore at the same load level, $SC_{0.68\%,50}$ achieved the height strain in comparison with other specimens which provided by 70, and 90 mm thick SHCC layer.

As listed in Table 6, the yielding loads of specimens $SC_{0.68\%,50}$, $SC_{0.68\%,70}$, and $SC_{0.68\%,90}$ are 300 kN, 305 kN, and 310 kN, respectively. The increase of the SHCC layer from 50mm to 90mm increased the yielding load by 3.3%. This result emphasizes that the enhancement due to the increase in the SHCC thickness is insignificant till yielding load and it does not worth the added cost of increasing SHCC layer.

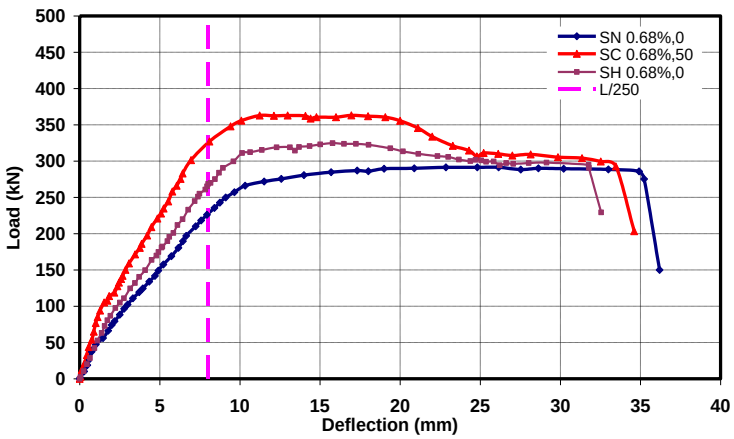

Fig. 10 Load-deflection curves for specimens of group (I).

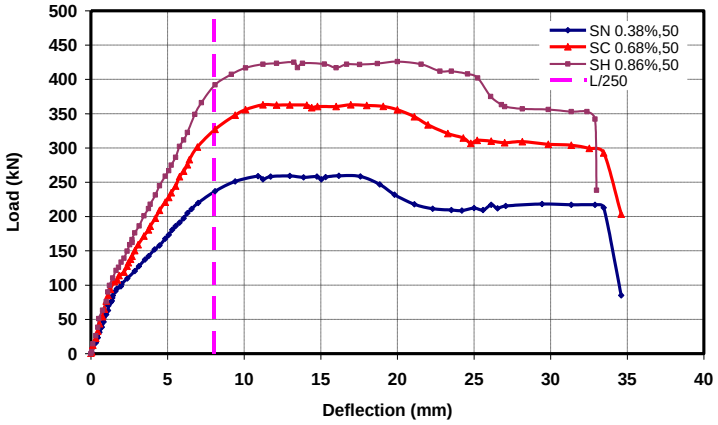

Fig. 12 Load-deflection curves for specimens of group (II).

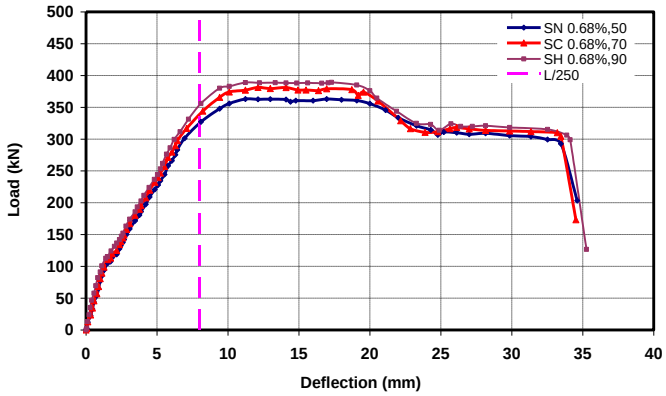

Fig. 13 Load-deflection curves for specimens of group (III).

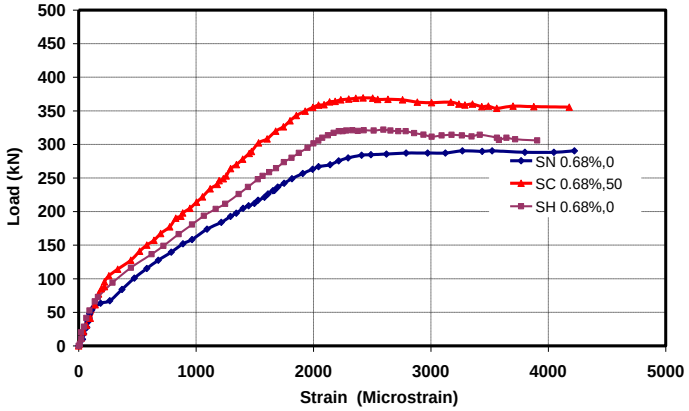

Fig. 14 load-strain response of the middle reinforcing bar for specimens of group (I).

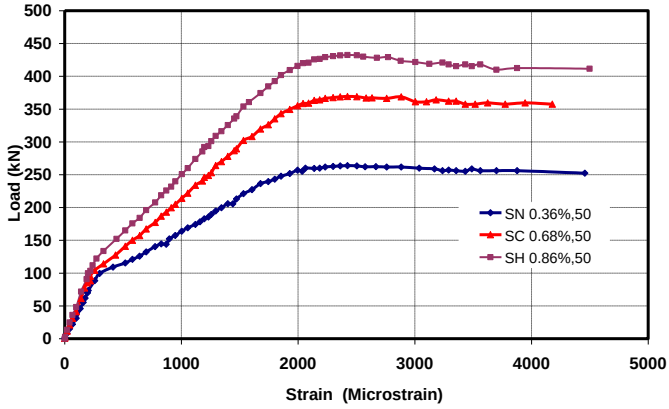

Fig. 15 load-strain response of the intermediate reinforcing bar for specimens of group (II).

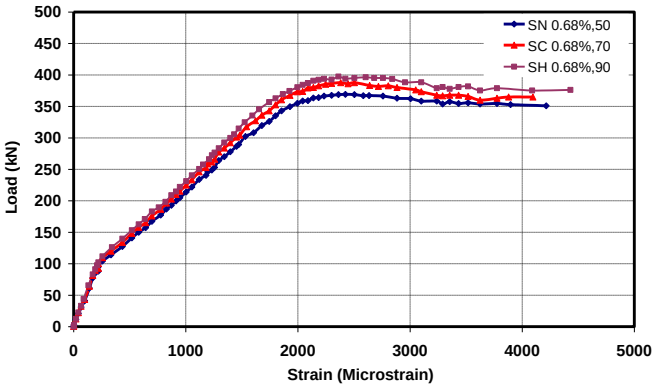

Fig. 16 load-strain response of the intermediate reinforcing bar for specimens of group (III) .

CRACKING BEHAVIOR

Both crack spacing and crack width affect the ultimate capacity as well as the durability of the bridge deck slab. Therefore, both of them have been discussed in details for the composite NSC/SHCC specimens as well as the control normal strength and high-performance concrete specimens.

CRACK SPACING

Figs. 17, 18 and 19show a schematic sketch for cracks propagation along the tension side of all specimens of the group (I) at different load levels. Specimen $SN_{0.68\%,0}$showed almost identical average crack spacing stating from the service load level up to the complete failure as depicted in Fig. 17, implying that new cracks occurred outward rather than between the former cracks. On contrary, with further loading, intermediate cracks were developed on the tension side of high-performance concrete specimen as depicted in Fig. 18. Furthermore, as indicated in Figs. 17 and 19, the flexural cracks in specimen $SN_{0.68\%,0}$ propagated more deeply toward the compression zone than that in specimen $SC_{0.68\%,50}$. This indicates that the neutral axis depth in specimen $SN_{0.68\%,0}$is further shifted up near the compression fiber. On the other hand, specimen $SC_{0.68\%,50}$exhibited flexural cracks with very short depths because the propagation of cracks was effectively restrained by fiber bridging at the crack surfaces.

As can be seen in Fig. 19, with increased load, the average crack spacing in specimen $SC_{0.68\%,50}$rapidly decreased and became constant after reaching the yielding load. In other words, the multiple cracking has reached the saturation state after yielding and few new cracks could form afterward. This observation is consistent with the theory of multiple cracking in fiber reinforced brittle matrix composites [32].

Effect of reinforcement ratio on crack spacing

The experimental observations showed that a similar cracking sequence was observed on the tension side of all specimens of group (II). The first crack appeared in the specimens once the cracking capacity of the SHCC was exhausted. With further increases in load, a multiple fine cracks formed along the span length of all specimens, and the formation of new cracks continued up to the failure of the specimen. Increasing the reinforcement ratio resulted in decrease the average crack spacing gradually with further loading, whereas the numbers of developed cracks were increased as depicted in Fig. 20. Furthermore, using of 0.86% reinforcement ratio enabled specimen $SC_{0.86\%,50}$to decrease the measured crack spacing to 21 mm, at service load level, which is about 60% of that achieved by specimen $SC_{0.38\%,50}$ which was had reinforcement ratio of 0.38%.

The enhancement in cracking behavior may be attributed to the increase in axial stiffness at cracks due to the contribution from reinforcement which enables the specimen to carry higher loads and consequently to form more cracks. The results seem to confirm that reinforcing the SHCC pre-cast layer with a high modulus of elasticity material such as steel reinforcement helps reduce the reinforcing fibers' stress just after cracking which in turn enables the specimen to carry higher loads (failure of tested specimens was controlled by the occurrence of the fibers rupture).

Effect of the thickness of the SHCC layer on crack spacing

All specimens of group (III) including specimens $SC_{0.68\%,50}$, $SC_{0.68\%,70}$, and $SC_{0.68\%,90}$, experienced almost equal flexural cracks spacing as depicted in Fig. 21. The experimental average cracks spacing observed at the service load level were 29 mm, 30 mm, 29 mm for specimens $SC_{0.68\%,50}$, $SC_{0.68\%,70}$, and $SC_{0.68\%,90,}$ respectively. The insignificant difference in cracks spacing, is consistent with the different code's provisions which consider the effective cracking depth is the quarter of the section depth, thus the increase in the SHCC thickness more than 50 mm almost does not affect cracks distribution of specimens $SC_{0.68\%,70}$, and $SC_{0.68\%,90}$ in comparison with specimen $SC_{0.68\%,50}$.Nevertheless, after yielding of internal reinforcement, the specimen $SC_{0.68\%,\ 50}$ showed deeper cracks depth in comparison with the other specimens of the group (III), and this refer to the increase of SHCC thickness precludes the rapid growth of the flexural cracks after yielding of the tension reinforcement, due to fiber bridging mechanism.

Table 6summarizes the different values of acting loads and the corresponding average crack spacing for all specimens at different stages of loading.

CRACK WIDTH

The durability of reinforced concrete structures can be enhanced by controlling the crack width. Also, the current codes limit the crack width in reinforced concrete structures for corrosion protection. Therefore, the crack width is a very important parameter to achieve a durable bridge deck. Fig. 22 shows the load-crack width response for test specimens of group (I). In addition, Table 7 summarizes the crack width of the tested specimens at the service, yielding, and at ultimate load levels.

For exposed RC buildings where the crack width has a significant influence on the durability and the appearance, different codes set a limiting value for maximum crack width. CEB-FIP and ECP 203-2017 codes set a limiting value of 0.2 mm. For comparison purpose, the measured crack widths at the service stage only are compared with the limiting value stipulated by CEB-FIP and ECP 203-2007.

As depicted in Fig. 22, cracks first appeared in the normal strength concrete deck once the cracking capacity of the concrete was exhausted. With further increases in the acting load, it was observed that the crack width increased rapidly and reached 0.24 mm at service load level. As reported in the Table 7, the use of HPC showed a reduction in the max crack width by about 40 %, at service stage level. On the other hand, the NSC/SHCC composite deck showed a superior cracking resistance, with finer and a higher number of cracks in comparison with those of the normal strength concrete and high-performance concrete decks.

The cracking response significantly influenced by the existence of fibers in SHCC layer. The utilization of SHCC with its superior tensile characteristics in NSC/SHCC deck effectively controlled the increase in crack width beyond the cracking occurrence. In fact, cracks started to appear when the load reached about 100 kN and till approximately 200 kN the cracks were not visible to the naked eyes. Moreover, the maximum crack width at the height level of tensile longitudinal steel bar for $SC_{0.68\%,0}$ remained below 0.08 mm till the service load level. This reduction was about 70% and 42% in comparison with $SN_{0.68\%,0}$ and $SH_{0.68,0}$,respectively. This means that NSC/SHCC decks are durable than NSC.As indicated in Fig. 22, it was observed that in the last stage of loading just after yielding of internal reinforcement, a significant increase in crack width of $SC_{0.68\%,50}$was recorded due to crack localization.

Effect of reinforcement ratio on crack width

Fig. 23shows that increasing the reinforcement ratio resulted indecrease the crack width. At a load level of 176 kN, service load of specimen $SC_{0.36\%,50,}$ the recoded values of crack width were 0.08 mm, 0.038 mm, and 0.033 mm for specimens $SC_{0.36\%,50}$, $SC_{0.68\%,50}$, and $SC_{0.86\%,50}$ respectively. This may be attributed to, increasing internal reinforcement for the NSC/SHCC composite deck, enhanced the strain hardening behavior of the SHCC pre-cast layer. Moreover, increasing the reinforcement ratio results in decrease the developed bar strain at the same load level. In fact, the crack width is in direct relation with bar strain. Thus, specimens $SC_{0.86\%,50}$and $SC_{0.68\%,50}$ exhibited lower crack widths compared to those of specimens $SN_{0.68\%,0}$ and $SC_{0.36\%,50}$.

Effect of the thickness of the SHCC layer on crack width

Figure 24shows load versus crack width response for all specimens of group (III). Group (III) consisted of three specimens $SC_{0.68\%,50}$, $SC_{0.68\%,70}$, and $SC_{0.68\%,\ 90}$ having different SHCC thickness; 50, 70, and 90 mm, respectively. However, cracks started to appear at a vertical load of about 100 kN, and after cracking, the crack width kept similar till reaching the yielding load of the internal reinforcement. With further loading, the increase of crack width slightly restricted within the increase of the SHCC layer thickness. Thus, specimen $SC_{0.68\%,50}$ was the most influenced specimen after yielding of the internal reinforcement. The SHCC matrix with its strain hardening behavior played the main role in limiting cracks growth, thus, with the increase in SHCC thickness the measured crack width decreased till the crack localization occurred. The measured crack width at a load level of about 240 kN (service load of specimen $SC_{0.68\%,50}$), were 0.08 mm, 0.08 mm, 0.07 mm for specimens $SC_{0.68\%,50}$, $SC_{0.68\%,70}$, and $SC_{0.68\%,\ 90}$, respectively.

Table 6: Acting load, corresponding average cracks spacing for all specimens at different loading stages.

Group No.	Specimen	P_s (kN)	S_s (mm)	P_y (kN)	S_y (mm)	S_u (kN)	S_u (mm)
Group (I)	$SN_{0.68\%,0}$	200	81	250	81	291	81
	$SH_{0.68\%,0}$	216	49	270	41	324	41
	$SC_{0.68\%,50}$	240	29	300	21	364	21
Group (II)	$SC_{0.38\%,50}$	176	35	220	24	259	22
	$SC_{0.86\%,50}$	292	21	365	16	425	16
Group (III)	$SC_{0.68\%,70}$	244	30	305	21	381	21
	$SC_{0.68\%,90}$	248	29	310	22	390	20

Ps = service load, S_s: average crack spacing corresponding to service load; P_y= yielding load, S_y= average crack spacing corresponding to yielding load; P_u= ultimate load, S_u: average crack spacing corresponding to ultimate load

Table 7: Acting load, corresponding major crack widthfor all specimens at different loading stages.

Group No.	Specimen	P (kN)	w_s (mm)	P_y (kN)	w_y (mm)	P_u (kN)	w_u (mm)
Group (I)	$SN_{0.68\%,0}$	200	0.24	250	0.27	291	0.64
	$SH_{0.68\%,0}$	216	0.14	270	0.19	324	0.54
	$SC_{0.68\%,50}$	240	0.08	300	0.12	364	0.45
Group (II)	$SC_{0.38\%,50}$	176	0.12	220	0.14	259	0.50
	$SC_{0.86\%,50}$	292	0.06	365	0.10	425	0.47
Group (III)	$SC_{0.68\%,70}$	244	0.08	305	0.11	381	0.44
	$SC_{0.68\%,90}$	248	0.07	310	0.11	390	0.43

P_s = service load; w_s= maximum crack width corresponding to service load; P_y= yielding load; w_y= maximum crack width corresponding to yielding load; P_u= ultimate load,;w_u= maximum crack width corresponding to ultimate load

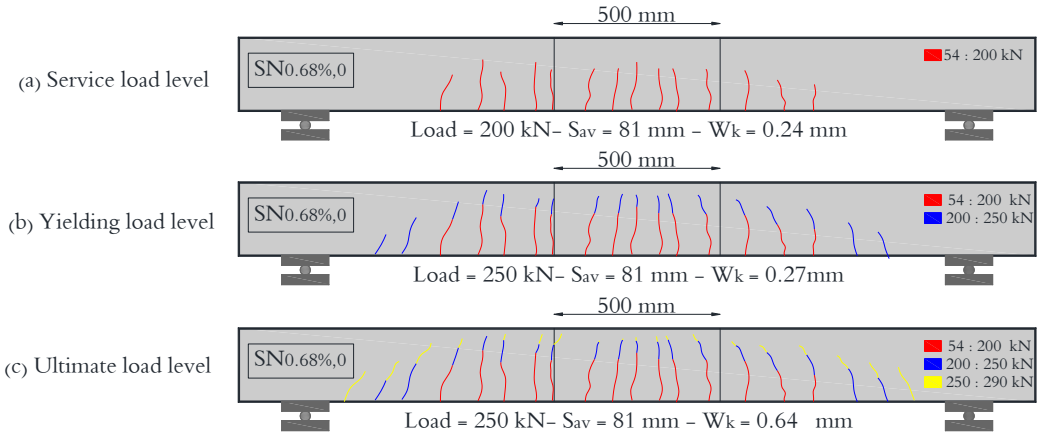

Fig. 17 Crack pattern of specimen $SN_{0.68\%,0}$ at service, yielding, and ultimate stages.

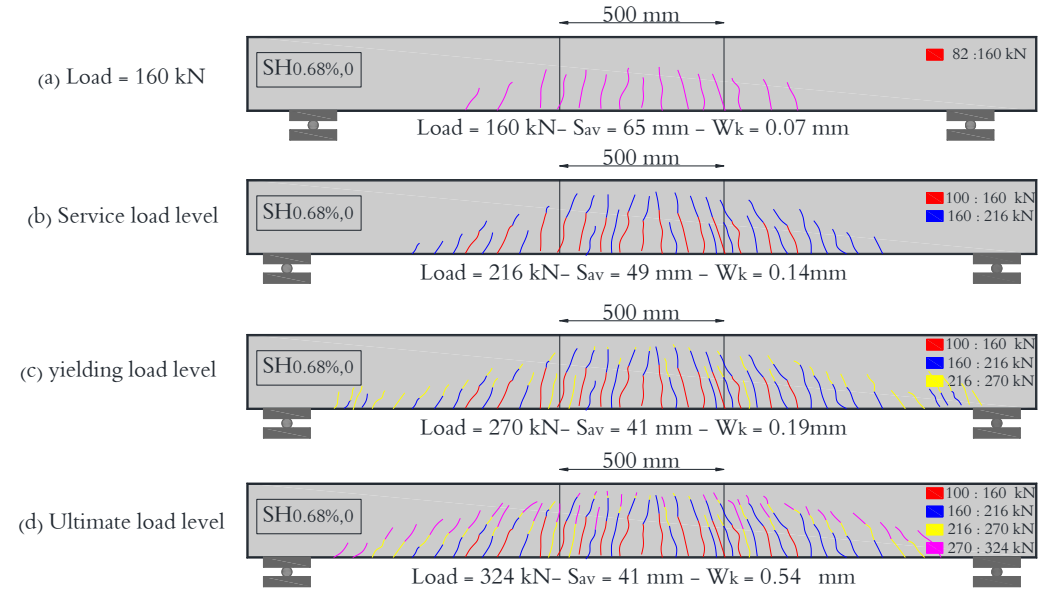

Fig. 18 Crack pattern of specimen $SH_{0.68\%,50}$ at 160 kN, service, yielding, and ultimate stages.

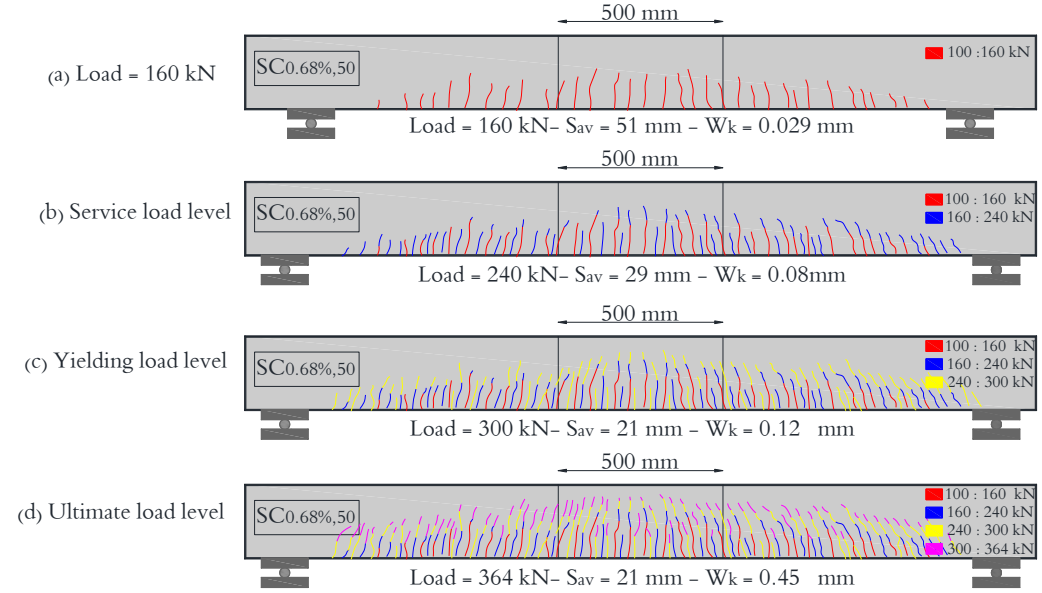

Fig.19 Crack pattern of specimen $SC_{0.68\%,50}$ at 160 kN, service, yielding, and ultimate stages.

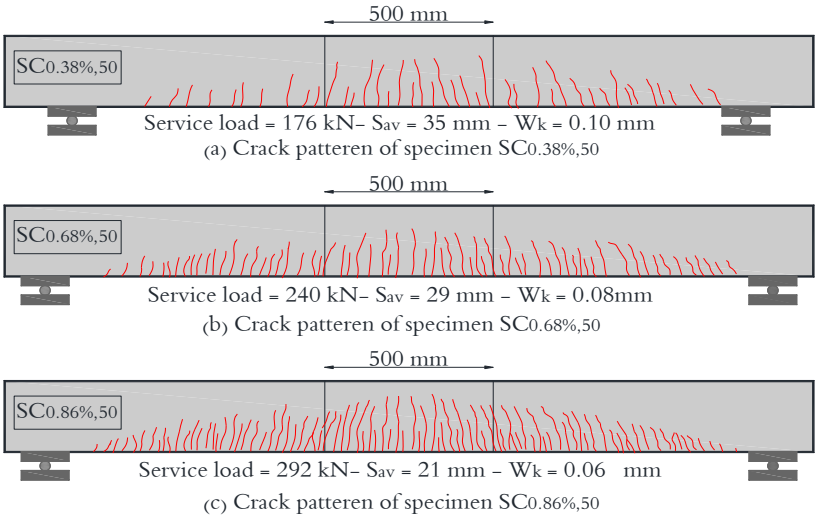

Fig. 20 Crack pattern for group (II), at service load level.

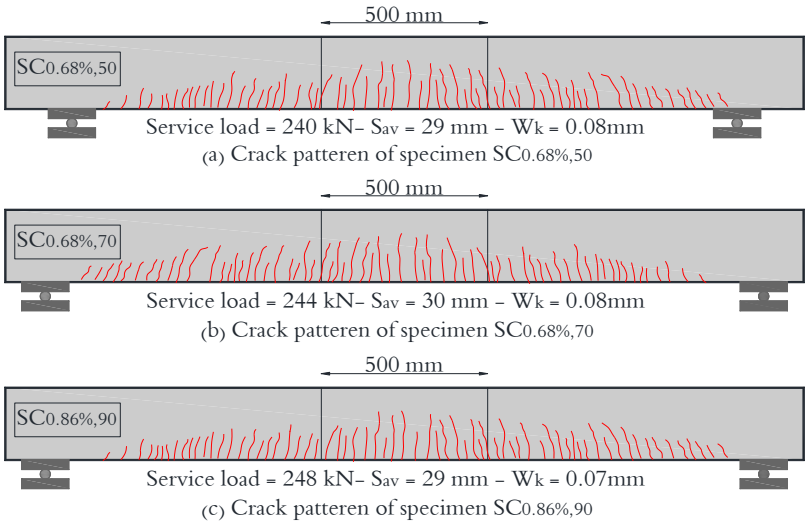

Fig. 21Crack pattern for group (III), at service load level.

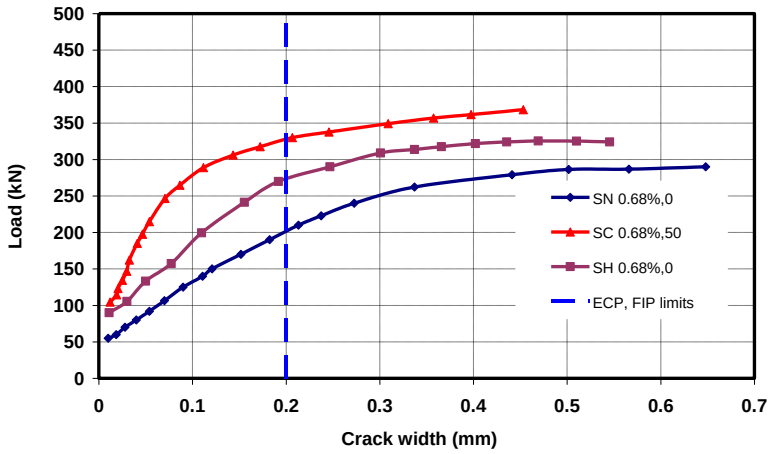

Fig.22load-crack width response for specimens of group (I).

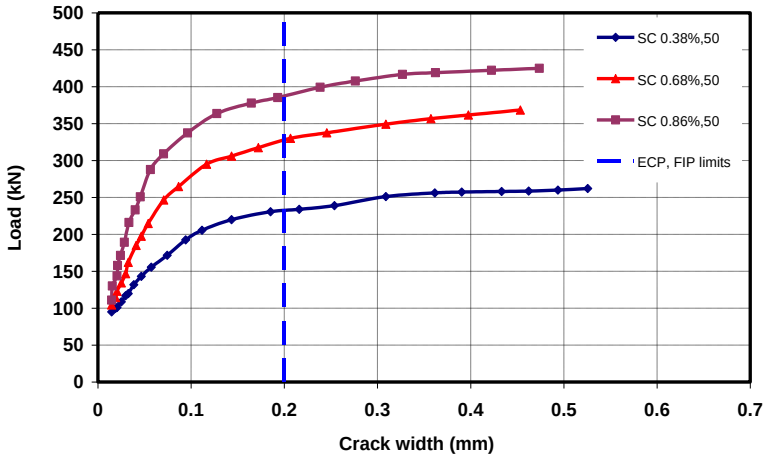

Fig. 23load-crack width response for specimens of group (II).

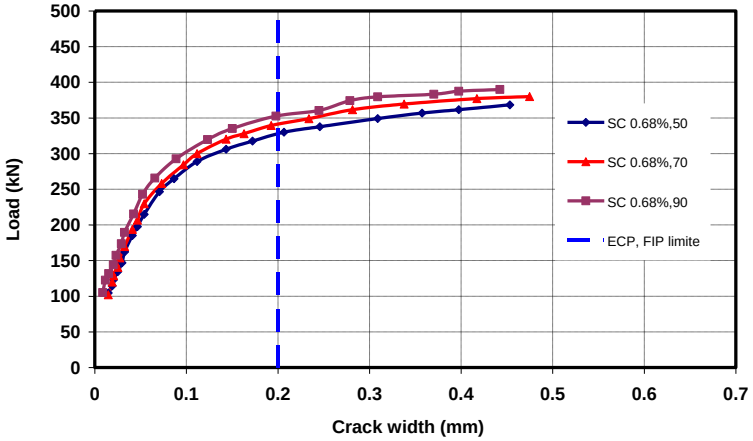

Fig. 24 load-crack width response for specimens of group (III).

CONCLUSIONS

This study aimed to propose and verify the competence of the composite NSC/SHCC section to be used in bridge construction in order to eliminate some drawbacks associated with using the traditional normal strength concrete. Based on the adopted concrete dimensions for both the NSC as well as the SHCC precast layers along with the internal reinforcement ratio, the following conclusions may be drawn:

1- Compared to the reference specimen that was made of a conventional reinforced concrete, the composite NSC-SHCC deck wherein precast reinforced SHCC layer with a thickness of 50 was placed at the tension side of the concrete deck gave substantial enhancement in flexural performance, post-cracking stiffness as well as yielding and ultimate load capacities of the deck. This enhanced performance is attributed to the formation of stable multiple micro-cracks in the SHCC layer as opposed to widening and localization of cracks in the conventional concrete deck .

2- Increasing the thickness of substrate precast SHCC layer higher than 50 mm showed slight enhancement in the flexural performance of the NSC/SHCC composite deck slab, which is not proportionate to the additional cost of the SHCC material. In addition, the increased thickness of the SHCC layer affects slightly the cracking characteristics of the NSC/SHCC composite section .

3- Increasing the reinforcement ratio of the main tensile steel resulted in insignificant enhancement on the cracking load, while it showed significant increase in the ultimate capacity.

4- The effect of internal main steel significantly affects the ultimate capacity, developed ductility, crack width and crack spacing.

REFERENCES

.

[1] Park H, Paulay T. Reinforced concrete structures. New York: John Wiley and Sons; 1975.
[2] Yun D et al. Crack width control of reinforced concrete one-way slabs utilizing expansive strain hardening cement-based composites (SHCCs). Fracture Mechanics of Concrete and Concrete Structures 2010; ISBN 978-89-5708-182-2
[3] EN 1992-1-1. Eurocode 2: design of concrete structures – Part 1-1: general rules and rules for buildings. Brussels: European Committee for Standardization (CEN); December 2004.
[4] CEB-FIP. Model code for concrete structures: CEB-FIP international recommendations. Paris: Comite Euro-International du Beton; 2010. p. 312.
[5] Egyptian code for design and construction of reinforced concrete structures (ECP 203-2017); 2017.
[6] American Concrete Institute. ACI, building code requirements for structural concrete (ACI 318-14) and commentary. Farmington Hills: ACI; 2014.
[7] Baah P. Cracking behaviour of structural slab bridge decks, Dissertation, university of Akron, December, 2014.
[8] Keller T. Fiber reinforced polymer materials in bridge construction. IABSE symposium, towards a better built environment - innovation, sustainability, information technology; 2002.
[9] Keller T, Gürtler H. In-plane compression and shear performance of FRP bridge decks acting as top chord of bridge girders. Compos. Struct. 2006; 72(2):151-162.
[10] Keller T, Schaumann E, Vallée T. Flexural behavior of a hybrid FRP and lightweight concrete sandwich bridge deck. Composites Part A 2007; 38(3): 879-889.
[11] Li VC. From micromechanics to structural engineering: the design of cementitious composites for civil engineering applications. JSCE J StructMechEarthqEng 1993;10:37–48.
[12] Li M, Li VC. High-early-strength ECC for rapid durable repair: material properties. ACI Mater J 2011;108:3–12.
[13] Li VC. Tailoring ECC for special attributes: a review.Int J ConcrStruct Mater 2012;6:135–44.
[14] Dhawale AW, Joshi VP. Engineered cementitious composites for structural applications.Int J Appl Innovation Eng Manage (IJAIEM) 2013;2:198–205.
[15] Fischer G, Li VC. Effect of fiber reinforcement on the response of structural members.EngFractMech 2007;74:25–272.
[16] Li VC. Reflections on the research and development of engineered cementitious composites (ECC). In: Proceedings of the JCI international workshop on ductile fiber reinforced cementitious composites (DFRCC) – application and evaluation, DFRCC-2002, Takayama, Japan; October 21–22, 2002. p. 1–21.
[17] Li VC. On engineered cementitiouscomposities (ECC), a review of the material and its applications. J AdvConcrTechnol 2003;1:215–30.
[18] Fukuyama H, Matsuzaki Y, Nakano K, Sato Y. Structural performance of beam elements with PVA-ECC. In: Reinhardt, Naaman A, editors. Proc of high performance fiber reinforced cement composites 3 (HPFRCC 3). Chapman & Hull; 1999. p. 531–42.
[19] Li VC, Fischer G. Reinforced ECC – an evolution from materials to structures. In: Proceedings on CD, Session 5, Paper K-13, Fib 2002, Osaka, Japan; 2002.
[20] Fischer G, Li VC. Deformation behavior of fiber-reinforced polymer reinforced engineered cementitious composite (ECC) flexural members under reversed cyclic loading conditions. ACI Struct J 2003;100:25–35.
[21] Fischer G, Li VC. Intrinsic response control of moment resisting frames utilizing advanced composite materials and structural elements. ACI Struct J 2003;100:166–76.
[22] Li VC, Li M. Durability performance of ductile concrete structures. In: Proceedings of the 8th international conference on creep, shrinkage and durability of concrete and concrete structures, Ise-Shima, Japan; 2008. p. 761–8.
[23] Sahmaran M, Li M, Li VC. Transport properties of engineered cementitious composites under chloride exposure. ACI Mater J 2007;104:604–11.
[24] Li M, Li VC. Cracking and healing of engineered cementitious composites under chloride environment. ACI Mater J 2011;108:333–40.
[25] Afefy H. M., Kassem N. M., Hussien M. and Taher S.F. Efficient strengthening of opened-joint for reinforced concrete broken slabs. Composite Structures 2016; Vol. 136, February, pp. 602-615.
[26] Afefy H.M., Kassem N.M. and Hussein M. Enhancement of flexural behavior of CFRP-strengthened reinforced concrete beams using engineered cementitious composites

transition layer. Structure and Infrastructure Engineering 2015; UK Vol. 11, No. 8, pp. 1042–1053.

[27] Hussein M., Kassem N.M., and Hassan A. An Innovative Efficient Strengthening For Reinforced Low Strength Concrete Cantilever Slabs. IOSR-JMCE 2015; Volume 12, Issue 5 Ver. I, PP 01-13.

[28] Kassem M., El-Shafeiy T., Hussein M., Afefy H. and Hassan A. Shear Behaviour of SHCC Dry Joints in Precast Construction International Conference on Advances in Structural and Geotechnical Engineering, ICASGE'17, Hurghada, Egypt, 27-30 March 2017.

[29] Bonaldo E, Oliveira de Barros JA, Lourenço PB. Efficient strengtheningtechnique to increase the flexural resistance of existing RC slabs. J ComposConstr 2008;12:149–59.

[30] Thomsen HH, Spacone E, Limkatanyu S, Camata G. Failure mode analysis ofreinforced concrete beams strengthened in flexure with externally bondedfiber-reinforced polymers. J Compos Constr 2004;8:123–31.

[31] Comite Euro-International du Beton-Federation International de la PreconStraente (CEB-FIP). Model code, Thomas Telford, London; 1990.

[32] Cong Lu, Jing Yu, Christopher K.Y. Leung, An improved image processing method for assessing multiplecracking development in Strain Hardening Cementitious Composites(SHCC) Cement and Concrete Composites 74 (2016) 191-200.